ACS OMEGA

http://pubs.acs.org/journal/acsodf

Article

Naked-Eye Detection of Hepatitis B Surface Antigen Using Gold Nanoparticles Aggregation and Catalase-Functionalized Polystyrene Nanospheres

Rubing Chen, Yongqin Hu, Meizhu Chen, Jia An, Ying Lyu, Yufei Liu,* and Dongling Li*

Cite This: *ACS Omega* 2021, 6, 9828−9833

Read Online

ACCESS | Metrics & More | Article Recommendations | Supporting Information

ABSTRACT: Developing rapid, efficient, highly sensitive, simple, stable, and low-cost virus marker detection products that are appropriate for basic facilities is of great importance in the early diagnosis and treatment of viruses. Naked-eye detection methods are especially important when medical testing facilities are limited. Polystyrene nanospheres (PSs) with catalytic and specific recognition functions were successfully developed by simultaneously modifying catalase and goat anti-hepatitis B surface antibodies on nanospheres. The modified PSs contributed significantly to the amplification of the signal. Via the specific antigen−antibody reaction, the bifunctional nanospheres could be captured on microplate and then catalyzed the decomposition of hydrogen peroxide to reduce chloroauric acid and synthesize gold nanoparticles (AuNPs). Due to the surface plasmon resonance of AuNPs, the solution color change could be observed with the naked eye and the limit of detection (LOD) was 0.1 ng/mL. Furthermore, the LOD observed with instrumentation was 0.01 ng/mL, which meant that a rapid, efficient, and highly sensitive method for the detection of hepatitis B surface antigens was successfully developed, and neither complex sample pretreatment nor expensive equipment was needed.

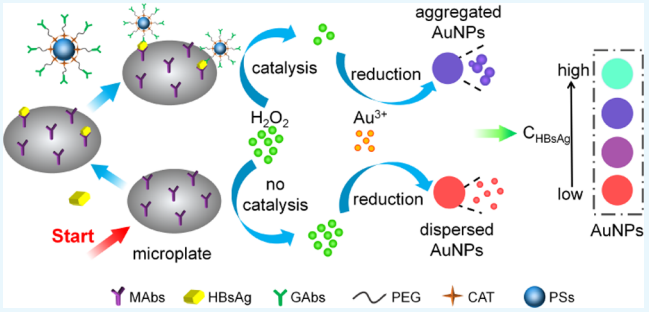

1. INTRODUCTION

Viral hepatitis is one of the most serious public health problems. For example, infection with hepatitis B virus (HBV) will lead to hepatitis B, which is endemic, widespread, and severely harmful. It can manifest in a variety of clinical types, such as chronic hepatitis, hepatocellular carcinoma, acute hepatitis, and cirrhosis,[1,2] leading to tens of thousands of deaths each year. At present, there is no effective treatment method for HBV at home or abroad, and patients can only be treated with nucleoside analogues or interferons to inhibit virus replication and worsening of the liver disease; nevertheless, for most patients, HBV cannot be eliminated. Therefore, early diagnosis of HBV is essential for the effective prevention and treatment of the disease.

The existing methods for detecting HBV include enzyme-linked immunosorbent assay (ELISA),[3] radioimmunoassay (RIA),[4] chemiluminescence immunoassay (CIA),[5] and electrochemical immunoassay (EIA).[6] Using commercially available ELISA to detect viruses is common because of the specific reaction of the antigen and the antibody and enzyme catalysis, but the shortcomings are also apparent; these include low sensitivity and easily missed inspections for low-level people. The RIA method is reliable and accurate, but its use suffers from problems related to health, waste disposal, and the need for expensive equipment. CIA cannot target a single compound but will react to a series of compounds, so its selectivity is poor. Additionally, the selectivity of EIA is usually poor. Therefore, the development of simple, sensitive, and rapid early clinical diagnosis and detection methods for HBV is essential for human health care.[7]

With the rise and development of nanotechnology, the unique physicochemical properties of nanomaterials have aided in the development of new methods for the sensitive detection of biological analytes, and various nanoparticles, including quantum dots,[8] nano-porphyrins,[9] and metal nanoparticles,[10] have been used in bioanalytical determinations. Colorimetric analysis methods based on the surface plasmon resonance (SPR) of gold nanoparticles (AuNPs), which do not require advanced instrumentation, have successfully attracted attention. Because AuNPs offer the advantages of good biocompatibility, unique optical and electronic properties, and relatively easy manufacturing, they are frequently used as carriers in various biomedical applications.[11] A range of biomacromole-

Received: January 28, 2021
Accepted: March 18, 2021
Published: March 30, 2021

cules, such as antibodies, oligonucleotides, and aptamers,[12] can functionalize AuNPs. Biomolecular interactions in biological processes can control their dispersion and aggregation. By monitoring the apparent color change caused by AuNPs, the detection of many kinds of (biological) molecules becomes easy,[12−19] and this provides an excellent platform for the colorimetric biosensor development. For example, Xiong et al. detected the Enterovirus 71 by the SPR of AuNPs with a limit of detection (LOD) equal to 0.65 ng/mL, which is much lower than the commercial ELISA detection (4.51 ng/mL).[20]

In this work, we advance a colorimetric detection scheme based on a specific antibody−antigen interaction, catalase-mediated growth, and aggregation of AuNPs. The method can detect hepatitis B surface antigen (HBsAg) directly and in a simple manner. As shown in Scheme 1, the capture antibody (mouse anti-HBsAg, MAbs) immobilized on a microplate specifically recognized and effectively captured HBsAg and then the HBsAg also combined with polystyrene nanospheres (PSs) that were modified with goat anti-HBsAg (GAbs) and catalase (CAT). The whole system formed an immune sandwich structure complex. More importantly, it also amplified the detection signal. Then, hydrogen peroxide (H_2O_2) decomposition was catalyzed by CAT on the complex and the remaining H_2O_2 reduced the Au^{3+} and further affected the morphology of the synthetic AuNPs, which resulted in a significant transformation of the solution color (from red to purple and further to blue). The corresponding absorbance change was proportional to the concentration of HBsAg. Therefore, the method achieves a highly sensitive, fast, efficient, and highly specific visual detection of HBsAg. Moreover, it does not require complex sample preparation, precision instruments, or specialized technical personnel; thus, it has broad prospects in clinical diagnosis, especially in resource-needy areas.

Scheme 1. Schematic Diagram of Naked-Eye Detection of HBsAg Using AuNPs Aggregation and Catalase-Functionalized PSs

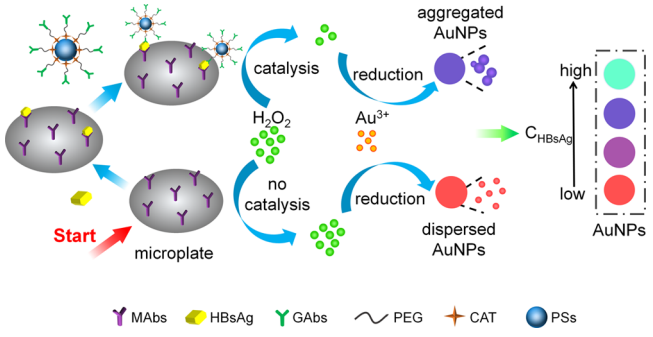

2. RESULTS AND DISCUSSION

2.1. Determination of the Feasibility of the Plan.

Scheme 1 shows the entire process for the visual detection of HBsAg. Only HBsAg was present, and the GAbs on the bifunctional nanospheres could bind to the captured HBsAg on the microplate. Subsequently, the CAT modified on the bifunctional nanospheres catalyzed the decomposition of H_2O_2; this, in turn, affected the morphology of the AuNPs synthesized with chloroauric acid, leading to the visually recognized change in the color of the solution. The higher the

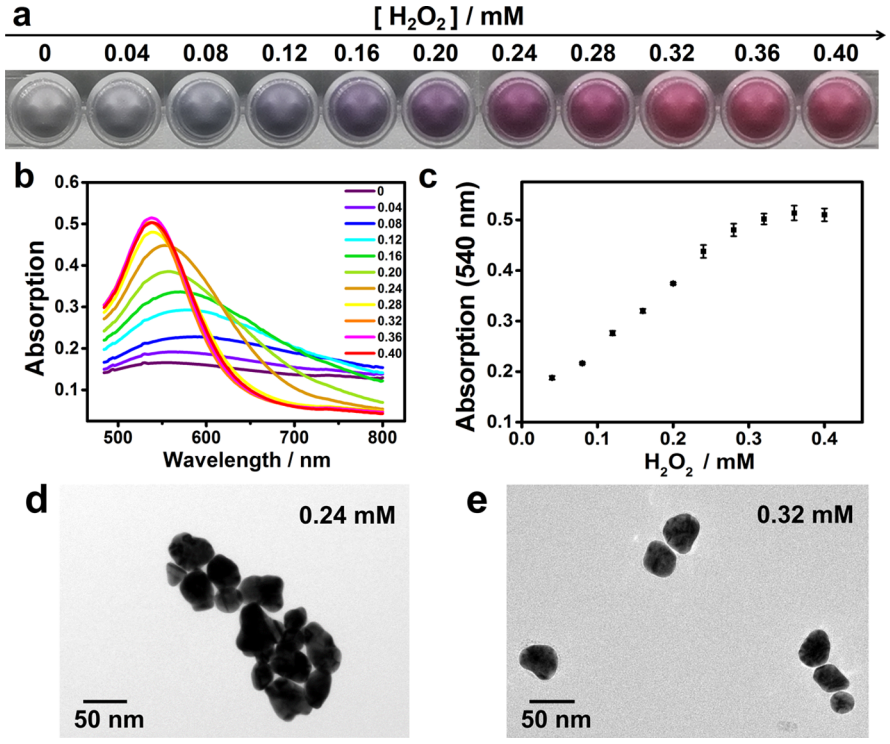

Figure 1. Relationship between the concentration of H_2O_2 and the morphology of AuNPs was built. A series of different concentrations of H_2O_2 were reacted with 0.34 mM chloroauric acid solution. (a) Color of the solution containing synthesized AuNPs after 30 min of reaction with different concentrations of H_2O_2. (b) UV−vis absorption characteristics of the abovementioned different AuNP solutions. When the H_2O_2 concentration was less than 0.28 mM, the AuNP local SPR peak red-shifted. (c) Absorbance of different AuNPs at 540 nm varied with the concentration of H_2O_2. (d,e) TEM images of AuNPs synthesized when the H_2O_2 concentrations were (d) 0.24 and (e) 0.32 mM.

https://doi.org/10.1021/acsomega.1c00507
ACS Omega 2021, 6, 9828−9833

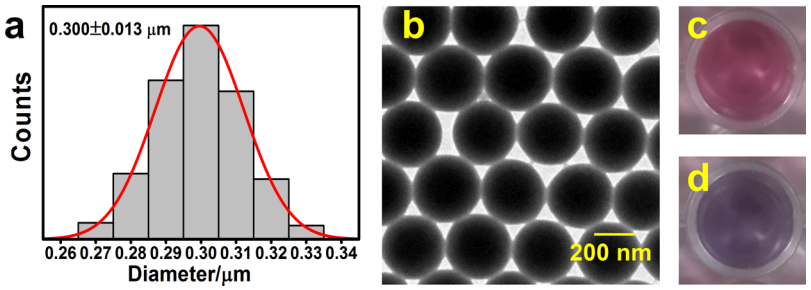

Figure 2. Characterization of PSs and verification of the feasibility of dual-functional PSs. (a) Corresponding size distribution of PSs. (b) TEM images of the PSs. In the presence of HBsAg, (c) when bifunctional nanospheres were not added, the color of the final solution was red, and (d) when bifunctional nanospheres were added, the color of the final solution was blue.

HBsAg concentration was, the greater the color change. Finally, fast, efficient, highly sensitive, and highly specific visual detection of HBsAg was achieved. To ensure the feasibility of the experimental design, it was crucial to prove that the H_2O_2 concentration could adjust the morphology and optical properties of the AuNPs synthesized with chloroauric acid.

When a series of different concentrations of H_2O_2 were reacted with 0.34 mM chloroauric acid solution, we observed a conspicuous transformation of the solution color from blue to purple to red (Figure 1a), which meant that the concentration of H_2O_2 did regulate the morphology of the synthesized AuNPs. This is because, when H_2O_2 reduces chloroauric acid, small AuNP seeds are first generated, and then, the generated seeds continue to grow. If the concentration of H_2O_2 is low, the nucleation rate for AuNPs will be slower than the growth rate, so it is easy to generate AuNPs with large particle sizes. If the concentration of H_2O_2 is high, the nucleation rate of AuNPs will be faster than the growth rate, and it is easy to generate many scattered AuNPs with small particle sizes. As shown in Figure 1b,c, when the concentration of H_2O_2 was less than 0.28 mM, the local SPR spectrum of the AuNPs broadened and redshifted to longer wavelengths. Additionally, transmission electron microscopy (TEM) imaging also confirmed that the final morphology of the synthesized AuNPs was strictly dependent on the concentration of H_2O_2 (Figures 1d,e and S1). In short, more viral antigens meant more enzymes were connected, less H_2O_2 remained after catalytic decomposition, the synthesized AuNPs were more agglomerated, and the solution color was blue, that is, the experimental scheme was feasible.

2.2. Optimization of Bifunctional Nanospheres. Based on the fact that the final morphology of synthesized AuNPs strictly depended on the concentration of H_2O_2, we designed an enzyme-catalyzed reaction in which CAT was used to decompose H_2O_2 and affect the morphology of the synthesized AuNPs. Additionally, to achieve rapid detection, we used PSs (approximately 300 nm in size) made in the laboratory as the carrier (Figure 2a,b). If GAbs, CAT, and PSs are reacted together, competition will occur between GAbs and CAT; GAbs is more competitive than CAT, which will affect the modification process. Therefore, we adopted a layer-by-layer modification method. Considering the issue of competitiveness, we first used CAT to occupy all the modification sites on the PSs and then used poly(ethylene glycol) (PEG) as the connecting arm between CAT and GAbs to increase the distance between them; this would reduce the steric hindrance and enhance the modification effect so that dual-function nanospheres (PSs@CAT@PEG@GAbs) with strong catalytic and specific recognition functions could be obtained. When an antibody molecule on the bifunctional PSs binds to an antigen molecule, all CAT on the complex will participate in the H_2O_2 catalytic reaction; therefore, the detection signal would be amplified and the sensitivity could also be improved. As shown in Figure 2c,d, in the presence of HBsAg, the addition of dual-functional nanospheres significantly affected the color of the final solution, which meant that the dual-functional nanospheres achieved the goal of detecting HBsAg. To ensure high detection sensitivity, the dual-function nanospheres needed to be optimized.

With 1 mg of PSs, the addition of different amounts of CAT for coupling resulted in different enzyme activities for the PSs@CAT obtained. As shown in Figure S2a, when 0.7 mg of CAT was used, the absorbance was the lowest of those observed, indicating that the color of the solution was the lightest and the concentration of H_2O_2 remaining after catalysis was the lowest, that is, the highest level of CAT was modified on the PSs and the best enzyme activity for PSs@CAT was observed. Similarly, as shown in Figure S2b,c, when 1 mg of PSs, 0.7 mg of CAT, 0.8 mg of PEG, and 30 μg of GAbs were fixed, the bifunctional nanospheres in the microplate could catalyze the most H_2O_2 and the concentration of H_2O_2 remaining was the lowest, so the solution exhibited the lightest color and the lowest absorbance. This meant that the coupling process of the dual-functional PSs had reached the optimal level, and subsequent testing could be carried out.

2.3. Detection of HBsAg. After obtaining the optimal dual-functional nanospheres, we sought to optimize each step of the detection to further improve the detection sensitivity. The specific optimization conditions are shown in Figure S3. Because the absorbances of the solutions in the experimental group at 540 nm were lower than that in the control group, it was easy to use these differences (ΔA_{540}) to distinguish successful and unsuccessful experiments. The larger ΔA_{540} was, the greater the color difference of the solution, the lighter the color of the solution in the experimental group with HBsAg added, which meant the detection sensitivity of HBsAg was higher under this experimental conditions. That is, the larger ΔA_{540} signified better conditions. The remaining detection conditions were optimized as follows: the concentration of the capture antibody (MAbs) coated on the microplate was 2 μg/mL, the reaction time for the specific binding of HBsAg and the MAbs was 75 min, the reaction time for the HBsAg that had been captured on the microplate specifically bound to the GAbs on the bifunctional nanosphere was 45 min, the reaction time to catalyze the decomposition of H_2O_2 by CAT on the dual-functional nanospheres binding to the microplate was 30 min, and, after decomposition, the reaction time for the remaining H_2O_2 reducing Au^{3+} to produce AuNPs was 10 min.

https://doi.org/10.1021/acsomega.1c00507
ACS Omega 2021, 6, 9828−9833

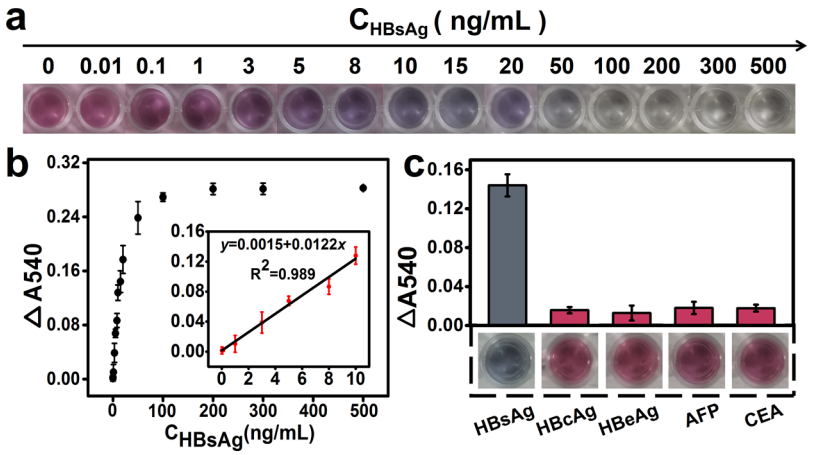

Figure 3. Proposed colorimetric method was used to detect HBsAg. With increasing HBsAg concentration, (a) change in the solution color and (b) change in absorbance at 540 nm (ΔA_{540}), inset: at low HBsAg concentrations, the concentration was linearly related to absorbance. Other common markers, such as hepatitis B core antigen (HBcAg), hepatitis B e antigen (HBeAg), carcinoembryonic antigen (CEA), and α-fetoprotein (AFP) antigen, were used as negative samples, and 2 mg/mL PBS−BSA solution was used as a control to verify the specificity of the method. (c) Color of the solution and the absorbance of the solution at 540 nm after addition of the samples.

Under these optimal conditions, different concentrations of HBsAg were tested. As shown in Figure 3a, when the HBsAg level increased, the number of combined bifunctional PSs increased, and the amount of H_2O_2 decomposed also increased, which greatly affected the morphology of the synthesized AuNPs. Additionally, the hue of the solution also transformed from red into purple, then into blue, and finally became colorless. To accurately measure the concentration of HBsAg, the decrease in the absorbance of the experimental group solution measured at 540 nm relative to that of the blank control (ΔA_{540}) is plotted in Figure 3b. As shown in Figure 3b, when the concentration of HBsAg increases, ΔA_{540} also increases, indicating that a linear relationship exists in the range 0.01 and 10 ng/mL, and the linear correlation coefficient (R^2) is 0.989 (inset of Figure 3b). The naked-eye LOD was 0.1 ng/mL and the instrumental LOD was 0.01 ng/mL, indicating that the immunocolorimetric assay in this paper could detect HBsAg with high sensitivity.

Furthermore, we compared the method proposed in this article with other traditional methods, such as ELISA, polymerase chain reaction (PCR), EIA, and so forth. As shown in Table 1, comprehensive sensitivity and instrument requirements indicated the superiority of the proposed method in naked-eye detection, which is suitable for resource-poor areas.

Table 1. Comparison of Different Detection Methods

method	detection object	LOD	references
ELISA	HBsAg	0.5 IU/mL	21
CIA	HBsAg	14 pg/mL	22
lateral flow	HBsAg	75 pg/mL	23
PCR	HBV DNA	2000 IU/mL	24
EIA	HBsAg	0.343 pg/mL	17

2.4. Specificity Verification. To evaluate the specificity of the method for the detection of HBsAg, other common markers, such as HBcAg, HBeAg, CEA, and AFP antigen, were used as negative samples, and 2 mg/mL PBS−BSA solution was used as a control. As shown in Figure 3c, the blue solution color caused by the aggregation of AuNPs could barely be observed in the presence of HBsAg. On the contrary, in the experiments with negative samples, because the markers could not combine with immune complexes, they were easily washed away when the microplate was washed, so the H_2O_2 added subsequently would not be catalyzed, and red scattered AuNPs were ultimately observed. Thus, we know that the color transformation of the solution was the result of the biospecific interaction between HBsAg and the corresponding specific antibody, indicating that our method has high specificity. Additionally, a microplate reader was used to verify the naked eye test results. Based on the decrease in absorbance at 540 nm (ΔA_{540}), the negative and positive samples could be easily distinguished. These results indicate that this method has high selectivity for the identification of HBsAg.

2.5. Detection of HBsAg in Spiked Serum Samples. To further evaluate the applicability of the immunoassay for detecting HBsAg in the human serum, different concentrations of HBsAg were added to the serum, which was diluted 40 times, and then, the detection was carried out under the optimal conditions. As shown in Table 2, recoveries of HBsAg at different concentrations (0.5−10 ng/mL) in the serum samples are between 93.44 and 104.67%, the average recovery is 100.66%, and the relative standard deviation (RSD) is between 0.04 and 3.61%, indicating that the colorimetric immunoassay is suitable for detecting HBsAg in serum samples and have great prospects for the application in actual clinical practice.

Table 2. Detecting HBsAg in Spiked Serum Samples by the Proposed Immunoassay

sample	spiked (ng/mL)	detected (ng/mL)	recovery (%)	RSD (%)
1	0.5	0.467	93.44	0.04
2	1	1.0467	104.67	0.57
3	4	4.161	104.04	3.61
4	8	7.863	98.29	2.95
5	10	10.284	102.84	2.98

https://doi.org/10.1021/acsomega.1c00507
ACS Omega 2021, 6, 9828−9833

3. CONCLUSIONS

In conclusion, the immunoassay method involving the CAT-mediated reduction of chloroauric acid to synthesize AuNPs has been successfully used to rapidly and visually detect HBsAg. It provides a simple way of reading results with the naked eye, using the amplification effect of the PSs and the enzyme-catalyzed reaction; this allows the detection of HBsAg with high efficiency, high sensitivity (instrumental LOD = 0.01 ng/mL), and high specificity, allowing the use of the method in resource-poor rural units. At the same time, the recovery levels in serum samples with our proposed method are between 93.44 and 104.67% and the RSD is between 0.04 and 3.61%, further indicating that the novel method has the great advantages of high specificity and low interference. The visual detection of HBsAg using immune amplification to catalyze the synthesis of AuNPs offers great potential for sensitive, reliable, convenient, and low-cost medical and point-of-care diagnosis.

4. MATERIALS AND METHODS

4.1. Materials. Microplates were purchased from JET. The ultrafiltration tube (50 k) was purchased from Bioground (Chongqing). HBsAg, HBcAg, HBeAg, enzyme-labeled antibody diluent, GAbs, and MAbs were purchased from Bai Aotong (Luoyang). 2-(4-Morpholino)ethanesulfonic acid (MES), catalase, and *N*-(3-dimethylaminopropyl)-*N*′-ethylcarbodiimide hydrochloride (EDC) were purchased from Sigma. NH_2−PEG−COOH was purchased from Peng Sheng Biological (Shanghai). The PSs−COOH (300 nm) was made in the laboratory. Chloroauric acid ($HAuCl_4$) was purchased from Macklin. BSA was purchased from BioFroxx. The remaining drugs were bought from Chron Chemicals. All the experiments used ultrapure water (18.2 MΩ cm).

4.2. Preparation of PSs@CAT@PEG@GAbs. First, the CAT must be purified because the purchased CAT solution is a suspension in which the CAT is not sufficiently dissolved. A part of the CAT stock solution was centrifuged, the supernatant was collected, and the precipitate was dispersed in 0.01 M PBS buffer (pH = 7.2) and centrifuged until the supernatant was colorless and transparent. After combining all the supernatants, an ultrafiltration tube was used to concentrate the samples, and the samples were washed with 0.01 M PBS buffer (pH = 7.2). Eventually, the remaining liquid in the ultrafiltration tube was adjusted to a constant volume and concentration, and the resulting liquid was used for the CAT experiment and stored at 4 °C.

The preparation of carboxylated PSs was described by Xie et al.[25] The preparation of PSs@CAT@PEG@GAbs was described by Hou et al., and some improvements were made.[26] PSs (1 mg), 0.7 mg of CAT, and 10 mL of 0.01 M PBS buffer were added to a round-bottom flask. After stirring at 25 °C for 1 h, 300 μL of the EDC solution was added and stirring was continued for 4 h. The mixture was washed once with 1× PBS buffer to obtain the PSs@CAT complex and then stored at 4 °C. The methods for the preparation of PSs@CAT@PEG and PSs@CAT@PEG@GAbs were the same as that for the PSs@CAT complex.

4.3. Detection of HBsAg. First, 100 μL of 2 μg/mL MAbs solution prepared with CB buffer was added to each well of the microplate and washed with PBST buffer after reacting at 37 °C for 2 h. Then, the plate was blocked with 1× PBS solution (containing 20 mg/mL BSA) for 1 h and washed with PBST buffer. It was then stored at 4 °C.

In a microplate coated with MAbs, 100 μL of HBsAg solution diluted with 2 mg/mL BSA solution (containing 0.05% Tween 20, prepared with 1× PBS buffer) was added to different concentrations in the sequence and then washed with PBST buffer after reacting at 37 °C for 75 min. Then, 20 μL of PSs@CAT@PEG@GAbs and 80 μL of enzyme-labeled antibody diluent were added. After reacting at 37 °C for 45 min, the cells were washed with PBST buffer 3 times, 1× PBS buffer twice, and water once. Subsequently, a certain amount of H_2O_2 diluted with 1 mM MES buffer (the pH of the buffer was adjusted to 6.50 with NaOH) was added to each well. After reacting at 37 °C for 30 min, the chloroauric acid solution was added to react for 30 min at 37 °C. A microplate reader was used to detect the absorbance of the solution at 540 nm. According to the difference in the absorbance between the control group and the experimental group, we established a linear relationship between the difference in the absorbance and the corresponding HBsAg concentration.

The specific steps of detection were the same as the steps for detecting HBsAg in PBS buffer.

4.4. HBsAg Detection in Human Serum. To verify the feasibility of this method for testing actual samples, HBsAg was added to a normal human serum (from a volunteer) diluted 40-fold. The added HBsAg concentrations were 0.5, 1, 4, 8, and 10 ng/mL.

■ ASSOCIATED CONTENT

Supporting Information

The Supporting Information is available free of charge at https://pubs.acs.org/doi/10.1021/acsomega.1c00507.

TEM images of the AuNPs formed with different concentrations of H_2O_2, optimal amounts of CAT, PEG, and GAbs used for 1 mg of PSs, and the optimization of specific detection steps (PDF)

■ AUTHOR INFORMATION

Corresponding Authors

Yufei Liu − *Key Laboratory of Optoelectronic Technology & Systems (Chongqing University), Ministry of Education, Chongqing 400044, China; Center for Intelligent Sensing Technology (CIST), College of Optoelectronic Engineering, Chongqing University, Chongqing 400044, China; Centre for NanoHealth, College of Science, Swansea University, Swansea SA2 8PP, U.K.;* orcid.org/0000-0003-2988-8843; Email: Yufei.Liu@cqu.edu.cn

Dongling Li − *Key Laboratory of Optoelectronic Technology & Systems (Chongqing University), Ministry of Education, Chongqing 400044, China*; Email: lidongling@cqu.edu.cn

Authors

Rubing Chen − *Key Laboratory of Optoelectronic Technology & Systems (Chongqing University), Ministry of Education, Chongqing 400044, China*

Yongqin Hu − *Key Laboratory of Optoelectronic Technology & Systems (Chongqing University), Ministry of Education, Chongqing 400044, China; Center for Intelligent Sensing Technology (CIST), College of Optoelectronic Engineering, Chongqing University, Chongqing 400044, China*

Meizhu Chen − *Key Laboratory of Optoelectronic Technology & Systems (Chongqing University), Ministry of Education, Chongqing 400044, China*

https://doi.org/10.1021/acsomega.1c00507
ACS Omega 2021, 6, 9828−9833

Jia An − *Key Laboratory of Optoelectronic Technology & Systems (Chongqing University), Ministry of Education, Chongqing 400044, China; Center for Intelligent Sensing Technology (CIST), College of Optoelectronic Engineering, Chongqing University, Chongqing 400044, China*

Ying Lyu − *Key Laboratory of Optoelectronic Technology & Systems (Chongqing University), Ministry of Education, Chongqing 400044, China*

Complete contact information is available at: https://pubs.acs.org/10.1021/acsomega.1c00507

Notes

The authors declare no competing financial interest.

■ ACKNOWLEDGMENTS

The project was supported by the Fundamental Research Funds for the Central Universities of China (grant no. 2019CDQYGD020 and no. 2019CDCGGD304), the National Key Research and Development Program of China (grant no. 2016YFE0125200) and National Natural Science Foundation of China (grant no. 61927818). We thank for the test platform provided by the Analytical and Testing Center of Chongqing University and Beijing Zhongkebaice Technology Service Co., Ltd.

■ REFERENCES

(1) Lavanchy, D. Worldwide epidemiology of HBV infection, disease burden, and vaccine prevention. *J. Clin. Virol.* **2005**, *34*, S1−S3.

(2) Ocama, P.; Opio, C. K.; Lee, W. M. Hepatitis B virus infection: current status. *Am. J. Med.* **2005**, *118*, 1413.

(3) Yamamoto, Y.; Saita, T.; Sogawa, R.; Ogata, K.; Yamamoto, Y.; Kimura, S.; Narisawa, Y.; Kimura, S.; Shin, M. Development of a sandwich enzyme-linked immunosorbent assay for the quantification of ponatinib in serum. *Anal. Biochem.* **2019**, *571*, 14−20.

(4) Franco-Martinez, L.; Tvarijonaviciute, A.; Martinez-Subiela, S.; Teles, M.; Tort, L. Chemiluminescent assay as an alternative to radioimmunoassay for the measurement of cortisol in plasma and skin mucus of Oncorhynchus mykiss. *Ecol. Indic.* **2019**, *98*, 634−640.

(5) Ehsani, M.; Chaichi, M. J.; Nezammeddin Hosseini, S. Comparison of CuO nanoparticle and CuO/MWCNT nanocomposite for amplification of chemiluminescence immunoassay for detection of the hepatitis B surface antigen in biological samples. *Sens. Actuators, B* **2017**, *247*, 319−328.

(6) Mandli, J.; Attar, A.; Ennaji, M. M.; Amine, A. Indirect competitive electrochemical immunosensor for hepatitis A virus antigen detection. *J. Electroanal. Chem.* **2017**, *799*, 213−221.

(7) Giljohann, D. A.; Mirkin, C. A. Drivers of biodiagnostic development. *Nature* **2009**, *462*, 461−464.

(8) Yang, X.; Xu, J.; Luo, N.; Tang, F.; Zhang, M.; Zhao, B. N,Cl co-doped fluorescent carbon dots as nanoprobe for detection of tartrazine in beverages. *Food Chem.* **2020**, *310*, 125832.

(9) Paolesse, R.; Nardis, S.; Monti, D.; Stefanelli, M.; Di Natale, C. Porphyrinoids for Chemical Sensor Applications. *Chem. Rev.* **2017**, *117*, 2517−2583.

(10) Yu, L.; Li, N. Noble Metal Nanoparticles-Based Colorimetric Biosensor for Visual Quantification: A Mini Review. *Chemosensors* **2019**, *7*, 53.

(11) Li, Y.; Schluesener, H. J.; Xu, S. Gold nanoparticle-based biosensors. *Gold Bull.* **2010**, *43*, 29−41.

(12) Saha, K.; Agasti, S. S.; Kim, C.; Li, X.; Rotello, V. M. Gold Nanoparticles in Chemical and Biological Sensing. *Chem. Rev.* **2012**, *112*, 2739−2779.

(13) Cordeiro, M.; Carlos, F. F.; Pedrosa, P.; Lopez, A.; Baptista, P. V. Gold Nanoparticles for Diagnostics: Advances towards Points of Care. *Diagnostics* **2016**, *6*, 43.

(14) Hu, J.; Wang, L.; Li, F.; Han, Y. L.; Lin, M.; Lu, T. J.; Xu, F. Oligonucleotide-linked gold nanoparticle aggregates for enhanced sensitivity in lateral flow assays. *Lab Chip* **2013**, *13*, 4352−4357.

(15) Kamińska, A.; Witkowska, E.; Winkler, K.; Dziecielewski, I.; Weyher, J. L.; Waluk, J. Detection of Hepatitis B virus antigen from human blood: SERS immunoassay in a microfluidic system. *Biosens. Bioelectron.* **2015**, *66*, 461−467.

(16) Kim, D. S.; Kim, Y. T.; Hong, S. B.; Kim, J.; Heo, N. S.; Lee, M.-K.; Lee, S. J.; Kim, B. I.; Kim, I. S.; Huh, Y. S.; Choi, B. G. Development of Lateral Flow Assay Based on Size-Controlled Gold Nanoparticles for Detection of Hepatitis B Surface Antigen. *Sensors* **2016**, *16*, 2154.

(17) Shourian, M.; Ghourchian, H.; Boutorabi, M. Ultra-sensitive immunosensor for detection of hepatitis B surface antigen using multi-functionalized gold nanoparticles. *Anal. Chim. Acta* **2015**, *895*, 1−11.

(18) Veigas, B.; Pedrosa, P.; Carlos, F. F.; Mancio-Silva, L.; Grosso, A. R.; Fortunato, E.; Mota, M. M.; Baptista, P. V. One nanoprobe, two pathogens: gold nanoprobes multiplexing for point-of-care. *J. Nanobiotechnol.* **2015**, *13*, 48.

(19) Wu, Y.; Guo, W.; Peng, W.; Zhao, Q.; Piao, J.; Zhang, B.; Wu, X.; Wang, H.; Gong, X.; Chang, J. Enhanced Fluorescence ELISA Based on HAT Triggering Fluorescence "Turn-on" with Enzyme-Antibody Dual Labeled AuNP Probes for Ultrasensitive Detection of AFP and HBsAg. *ACS Appl. Mater. Interfaces* **2017**, *9*, 9369−9377.

(20) Xiong, L.-H.; He, X.; Xia, J.; Ma, H.; Yang, F.; Zhang, Q.; Huang, D.; Chen, L.; Wu, C.; Zhang, X.; Zhao, Z.; Wan, C.; Zhang, R.; Cheng, J. Highly Sensitive Naked-Eye Assay for Enterovirus 71 Detection Based on Catalytic Nanoparticle Aggregation and Immunomagnetic Amplification. *ACS Appl. Mater. Interfaces* **2017**, *9*, 14691−14699.

(21) van den Berg, L. M.; Ribeiro, C. M. S.; Zijlstra-Willems, E. M.; de Witte, L.; Fluitsma, D.; Tigchelaar, W.; Everts, V.; Geijtenbeek, T. B. H. Caveolin-1 mediated uptake via langerin restricts HIV-1 infection in human Langerhans cells. *Retrovirology* **2014**, *11*, 123.

(22) Sabouri, S.; Ghourchian, H.; Shourian, M.; Boutorabi, M. A gold nanoparticle-based immunosensor for the chemiluminescence detection of the hepatitis B surface antigen. *Anal. Methods* **2014**, *6*, 5059−5066.

(23) Shen, J.; Zhou, Y.; Fu, F.; Xu, H.; Lv, J.; Xiong, Y.; Wang, A. Immunochromatographic assay for quantitative and sensitive detection of hepatitis B virus surface antigen using highly luminescent quantum dot-beads. *Talanta* **2015**, *142*, 145−149.

(24) Price, H.; Dunn, D.; Zachary, T.; Vudriko, T.; Chirara, M.; Kityo, C.; Munderi, P.; Spyer, M.; Hakim, J.; Gilks, C.; Kaleebu, P.; Pillay, D.; Gilson, R.; Grp, D. V. Hepatitis B serological markers and plasma DNA concentrations. *AIDS* **2017**, *31*, 1109−1117.

(25) Xie, H.-Y.; Zuo, C.; Liu, Y.; Zhang, Z.-L.; Pang, D.-W.; Li, X.-L.; Gong, J.-P.; Dickinson, C.; Zhou, W. Cell-Targeting Multifunctional Nanospheres with both Fluorescence and Magnetism. *Small* **2005**, *1*, 506−509.

(26) Hou, Y.; Cai, G.; Zheng, L.; Lin, J. A microfluidic signal-off biosensor for rapid and sensitive detection of Salmonella using magnetic separation and enzymatic catalysis. *Food Control* **2019**, *103*, 186−193.